

## Theme Issue Article

# Binding between heparin and the integrin VLA-4

Martin Schlesinger; Dirk Simonis; Patrick Schmitz; Juliane Fritzsche; Gerd Bendas

Department of Pharmacy, Rheinische Friedrich Wilhelms University, Bonn, Germany

### Summary

Heparin possesses antimetastatic effects that were related to various molecular mechanisms beyond anticoagulant activities. The ability of heparin to interfere with the function of adhesion receptors in the metastatic course appears as a promising therapeutic approach. This refers to numerous findings that heparin attenuates metastasis in a selectin-dependent manner. We recently demonstrated that heparin interferes with the integrin VLA-4 on murine melanoma cells binding to VCAM-1. To confirm this activity and to obtain further insight into molecular recognition of heparin by VLA-4, we investigated the inhibition of VLA-4 mediated binding of human melanoma MV3 cells to immobilised VCAM-1 by different heparins. The size of heparin has an important impact on inhibition. Unfractionated heparin (UFH) and tinzaparin, a low-molecular-weight heparin (LMWH) representing a mean of about 18–20 monomers, displayed high

inhibitory activity. Fractionating tinzaparin to 14–18 monomers reduced inhibition slightly, while the pentasaccharide fondaparinux was without effects. To confirm molecular recognition of tinzaparin by VLA-4, a surface acoustic wave-biosensor was applied. AVLA-4 containing membrane preparation of MV3 cells was immobilised at the sensors to allow for detection of kinetic binding constants of tinzaparin compared to VCAM-1. Tinzaparin binds to VLA-4 with affinity in the low micromolar range ( $4.61 \times 10^{-6}$  M), which clearly indicates specific molecular recognition. Furthermore, tinzaparin displays a nearly identical  $k_{\text{off}}$  compared to VCAM-1 ( $5.13 \times 10^{-3} \text{ s}^{-1}$  versus  $3.44 \times 10^{-3} \text{ s}^{-1}$ ) which is evident for interference with the ligand binding. The data provide evidence for a direct confirmation of heparin binding to VLA-4 and thus, contribute to understand the antimetastatic activity of heparin.

### Keywords

Heparin, melanoma cell adhesion, VLA-4, antimetastatic activity

Thromb Haemost 2009; 102: 816–822

### Introduction

Tumor cell metastasis may lead to serious complications in cancer. Thus, its effective treatment is required to inhibit tumor growth or to improve survival of cancer patients. The mechanisms of metastasis are complex and versatile including multiple steps that allow tumor cells to disseminate and to proliferate. Cell adhesion molecules (CAMs) are crucially involved in the metastatic cascade promoting cell-cell, cell-endothelium, cell-platelet, and cell-extracellular matrix (ECM) interactions. Thus, anti-adhesion strategies appear as promising approaches in oncology (1). The selectins, a class of carbohydrate-binding proteins, recognise several structures on tumor cell surfaces, leukocytes, platelets, and endothelial cells, thereby creating multiple binding possibilities. This leads to the formation of microemboli enabling the tumor cells to survive and to arrest in the microvasculature (2). Beside selectins, integrins and their li-

gands of the immunoglobulin superfamily participate in adhesive interactions between tumor cells and the endothelium, such as the integrin  $\alpha 4 \beta 1$  (very late activation antigen-4, VLA-4) and vascular cell adhesion molecule-1 (VCAM-1). Both, the selectin and the VLA-4 mediated binding pathway contribute to experimental metastasis of tumor cells bearing the respective ligands/receptors, such as malignant melanoma cells (3, 4), whereas their activities are even of clinical relevance (5). We and others were able to show that especially melanoma cells utilise the VLA-4/VCAM-1 binding pathway to directly adhere to the endothelium, whereas selectins are involved in forcing platelet-cell interactions and in polymorphnuclear neurophils (PMNs)-facilitated extravasation (6, 7).

For prophylaxis and treatment of thrombosis, heparin has been the drug of choice for several decades. With the findings that – in addition to the prevention of thromboembolism – heparin prolongs the survival of cancer patients (8), research is going

Correspondence to:  
Prof. Dr. Gerd Bendas  
Department of Pharmacy  
Rheinische Friedrich Wilhelms University Bonn  
An der Immenburg 4  
53121 Bonn, Germany  
Tel.: +49 228 735250, Fax: +49 228 734692  
E-mail: gbendas@uni-bonn.de

Financial support:  
This work was in part supported by grants from Deutsche Forschungsgemeinschaft (GRK 677 to JF, DS, and MS).

Received: January 26, 2009  
Accepted after major revision: June 28, 2009

Prepublished online: September 15, 2009  
doi:10.1160/TH09-01-0061

on to identify the molecular mechanisms. Currently assumed heparin actions beside anticoagulation are (i) inhibition of P- and L-selectin, (ii) inhibition of angiogenesis via stimulation of tissue factor pathway inhibitor (TFPI)-release, (iii) modulation of growth factor binding, and (iv) inhibition of heparanase enzymatic activity (9–12). Taking into account that VLA-4 plays a dominant role in melanoma cell adhesion, its inhibition seems to be essential to decrease metastasis. In a recent study, we showed for the first time that the adhesion of murine B16F10 melanoma cells to VCAM-1 could be inhibited by heparin *in vitro* and suggest VLA-4 as a novel heparin target (6). Although a combination of different techniques was used, the final proof of a direct binding between heparin and VLA-4 was lacking. Indeed, there are observations of others, who refer to the binding ability of heparin to the integrins  $\alpha$ IIb $\beta$ 3,  $\alpha$ M $\beta$ 2 (Mac-1),  $\alpha$ X $\beta$ 2 (gp 150,95) (13–15) and to specific integrins on a transfected erythroleukemic cell line in dependence on the integrin  $\beta$ -subunit (16). However, none of these studies was associated with the antimetastatic properties of heparin.

To strengthen our hypothesis of heparin/VLA-4 interactions, the present study investigates the inhibitory effects of different heparins on human MV3 melanoma cell adhesion to VCAM-1 under flow conditions. Unfractionated heparin (UFH), low-molecular-weight heparin (LMWH) tinzaparin, a fraction of tinzaparin representing a proportion of 14, 16, and 18 monosaccharides as well as fondaparinux were included. The results show a clear dependence of the inhibitory capacity on the molecular weight of heparin.

To detect heparin/VLA-4 binding on a molecular level, a surface acoustic wave (SAW) biosensor was applied. On basis of the piezoelectric properties, mass changes on the surface of sensors can be detected as phase shift of an applied acoustic wave. For detailed principles of measurement, the underlying physical mechanisms, and the mathematical bases for determination of kinetic binding constants the reader is referred to (17) and for several applications to (18–20). SAW-based cell experiments have been applied mainly using bacteria, bacteriophages, and yeasts (21–23), but also mammalian cell interactions (24, 25).

In the present study, the SAW method was applied for the first time at adhesion receptor mediated interactions, i.e. between VLA-4 expressing MV3 cells and VCAM-1. By immobilising a membrane preparation of MV3 cells on the sensor surface we were able to determine binding kinetics of VCAM-1 and tinzaparin to VLA-4 and thus, confirmed heparin binding to VLA-4.

Therefore, VLA-4 is coming into light as an attractive target for the antimetastatic effects of heparin leading to a decrease of human melanoma cell adhesion.

## Materials and methods

### Cell culture

All cell lines were cultured at 37°C in humidified atmosphere containing 5% CO<sub>2</sub>.

The human melanoma cell line MV3 was grown in RPMI 1640 supplemented with 10% (v/v) fetal calf serum (FCS). For subcultivation, MV3 were detached at 80–90% confluency using EDTA-solution (0.2 g/l EDTA  $\times$  4 Na) for 3 min at 37°C. All

reagents were from Sigma-Aldrich Chemie GmbH (Taufkirchen, Germany).

Human umbilical vein endothelial cells (HUVECs) were cultured in Endothelial Cell Growth Medium. Subcultivation was performed at 60–80% confluency using DetachKit in accordance with the provided protocol. HUVECs and all reagents were obtained from PromoCell GmbH (Heidelberg, Germany).

### Antibodies and adhesion molecules

The humanised anti-VLA-4 ( $\alpha$ -chain) mAb natalizumab was kindly provided from Biogen Idec GmbH (Ismaning, Germany). Goat anti-human IgG-horseshoe peroxidase (HRP) was purchased from Antibody Online (Aachen, Germany).

Function-blocking anti-human P-selectin mAb and recombinant human VCAM-1 Fc (human IgG<sub>1</sub>) chimera were obtained from R&D Systems GmbH (Wiesbaden-Nordenstadt, Germany).

### Sulfated polysaccharides

UFH 1 was kindly provided by Dr Annamaria Naggi (“G Ronzoni” Institute for Chemical and Biochemical Research, Milan, Italy). UFH 2 (Heparin-Natrium 5000 ratiopharm®) was purchased from Ratiopharm GmbH (Ulm, Germany), tinzaparin was from LEO Pharma GmbH (Neu-Isenburg, Germany) and fondaparinux from Sanofi-Aventis GmbH (Frankfurt/M, Germany). The fraction of tinzaparin consisting of 14, 16, and 18 monosaccharides was isolated by size-exclusion chromatography on Biogel-P10 as described by Bisio et al. in the present issue of T.H.

### Flow chamber assay

Adhesive interactions of MV3 cells with VCAM-1 Fc chimera or HUVECs were determined under physiological flow conditions. Glass slides containing 0.2  $\mu$ g VCAM-1 or confluent HUVECs, stimulated with 50 ng/mL human tumor necrosis factor (TNF)- $\alpha$  (Sigma-Aldrich GmbH, Taufkirchen, Germany) for 4 to 6 hours, were incorporated into a parallel plate flow chamber as described in detail in our previous investigations (6, 26). Briefly, the flow chamber was mounted onto an inverted microscope. PBS (pH 7.4) as flow medium was driven by hydrostatic pressure at a shear rate of about 200 s<sup>-1</sup>. Experiments were performed after treatment of 1 $\times$ 10<sup>6</sup> MV3 cells suspended in FCS-free RPMI 1640 with 1 mM Mn<sup>2+</sup> for 5 min at 37°C (stimulated cells) in comparison to untreated cells. To determine the contribution of P-selectin on MV3 cell interaction with HUVECs, 10  $\mu$ g of a function-blocking anti-human P-selectin mAb were mixed with 1 $\times$ 10<sup>6</sup>/100  $\mu$ L MV3 cell suspension and put into the flow chamber.

For inhibition experiments, heparin preparations and natalizumab were used at 500  $\mu$ g (according to 150 IU  $\approx$  1 mg) and 5  $\mu$ g, resp., and compared with the inhibitor-free control experiment (cells in FCS-free medium only). The substances were added to 100  $\mu$ L stimulated MV3 cells and incubated for 5 min at 37°C prior to injection into the flow system.

Adhesion behavior of the MV3 cells was monitored over a period of 5 s. Video sequences were captured with the camera CSC-795 (Pacific Corporation, Tokyo, Japan) and analysed with the software Imagoquant MultiTrack-AVI-2 (Mediquant GmbH, Lützen, Germany).

### SAW biosensor measurements

Biosensor investigations were performed using a S-Sens™ K5 surface acoustic wave biosensor supplied by Biosensor GmbH, Bonn, Germany.

### Immobilisation of VCAM-1 and natalizumab on the SAW sensor

Gold-coated sensors (Biosensor) were incubated in a solution of 11-mercaptoundecanoic acid (10 mM) in ethanol abs. forming a self-assembled monolayer by binding of the sulfur headgroups to the gold surface. The carboxyl groups were activated with 200 mM *N*-ethyl-*N*-(dimethylaminopropyl)-carbodiimide (EDC) and 50 mM *N*-hydroxysuccinimide (NHS) to bind 50 µg/mL natalizumab and VCAM-1, respectively, forming carboxylamides. An excess of activated unreacted NHS esters was blocked by 1 M ethanolamine (pH 8.5). The amount of bound protein was determined using the protocol described in (17).

### Cell binding experiments to VCAM-1 and natalizumab

After immobilisation of VCAM-1 and natalizumab, respectively, a baseline equilibration in PBS containing 1 mM Ca<sup>2+</sup> and Mg<sup>2+</sup> was performed for 30 min. In that time, 5×10<sup>6</sup> MV3 cells were suspended in 1 mL running buffer containing 1 mM Mn<sup>2+</sup>. The number of injected cells was optimised based on the findings that 1×10<sup>3</sup> cells was the minimum to detect binding events, while numbers >1×10<sup>6</sup> did not lead to increased binding. The flow rate to ensure sufficient time for cell-ligand interaction and to prevent unspecific binding due to sedimentation was 100 µL/min.

For inhibition experiments, 500 µg tinzaparin in 10 µL buffer were added to 1×10<sup>6</sup> cells, injected into the biosensor system and rinsed either over immobilised VCAM-1 or natalizumab. Binding of cells with or without inhibition was measured as shift of phase. Since the penetration depth of a love wave sensor is restricted to the near sensor surface, only mass changes caused by ligand-receptor/antibody interactions close to the sensor surface were detected without balancing the whole cell.

### Preparation of membrane vesicles

MV3 cells were harvested from 80% confluent grown cell dishes. Cell membrane vesicles were prepared according to the protocol described in detail in (27). All steps were performed at 4°C. Membrane vesicles were homogenised using a Potter-Elvehjem homogenisator. The protein yield was determined in an amido black-protein assay (28). Presence of VLA-4 was determined applying a SDS-page under non-reducing conditions. Proteins from the gel were plotted on a polyvinylidene difluoride membrane at 100 V, 350 mA for 60 min. Unspecific binding sites on the membrane were blocked using a solution of skim-milk protein (5%) in TBS with 0.2% Tween. VLA-4 was detected using natalizumab and anti-human IgG-HRP as secondary antibody. Chemoluminescence was detected after treating the membrane with Immobilon™-Western Chemoluminescent Kit (Millipore Corporation, Billerica, USA) according to the manufacturer's protocol.

### Immobilisation of membrane vesicles on SAW sensors

Gold-coated SAW sensors were inserted into an aqueous solution of 1-β-thiogluco-10 (10 mM) over night to form an adhesion

layer for the membrane vesicles. After rinsing briefly with ethanol and drying under a stream of nitrogen, the sensor chips were inserted into the flow chamber of the SAW biosensor and a baseline equilibration was performed for 30 min in PBS containing 1 mM Ca<sup>2+</sup> and Mg<sup>2+</sup>. The amount of injected membrane vesicles was defined by a dilution series of the membrane vesicles. A 1:10-dilution of the membrane vesicles in running buffer was assumed to be appropriate after detection experiments using VLA-4 binding antibody natalizumab.

### Determination of kinetic binding constants of VCAM-1, tinzaparin, and fondaparinux

VCAM-1, tinzaparin, and fondaparinux, resp., were injected in dilution series between 10<sup>-12</sup> M and 10<sup>-3</sup> M to interact with the immobilised membrane vesicles. Association and dissociation events were detected as phase shifts indicating binding and unbinding events at the membrane vesicle surface. Kinetic binding constants were calculated from the slopes of the obtained curves applying a 1:1-binding model.

### Statistics

Data represent means ± standard deviations of at least three independent experiments. Comparisons were performed by the unpaired Student's t-test (\*p<0.05, \*\*p<0.01, \*\*\*p<0.001).

## Results and discussion

### VLA-4-mediated binding of MV3 melanoma cells to VCAM-1 can be blocked by different heparins – Insight into structural requirements

In order to simulate the situation of tumor cell adhesion to the endothelium, the binding of MV3 cells to confluent, TNF-α-treated HUVECs was determined under physiological flow conditions. TNF-α induces VCAM-1 expression on HUVECs in a time-dependent manner with near maximal expression being seen after 4 to 6 hours of stimulation (29). It can be noticed that Mn<sup>2+</sup>-treatment enhanced cell adhesion in a statistically significant extent from 76.5% ± 6.9% up to 87.3% ± 5.8% at 4 s (Fig. 1A). Beside chemokines, the treatment with Mn<sup>2+</sup> is an experimentally accepted way of activation of almost all integrins. Thus, the Mn<sup>2+</sup>-induced increased cell adhesion points to a contribution of integrin-mediated binding pathways. Since the VLA-4-blocking mAb natalizumab was able to decrease cell binding (76.0% ± 4.2%) to the level of unstimulated cells, an explicit VLA-4 dependency can be assumed. VLA-4 positivity of MV3 was ensured by flow cytometry (data not shown).

In addition to VCAM-1, a variety of other cell adhesion molecules are expressed/induced on HUVECs, such as P-selectin. MV3 cells possess binding ability to P-selectin Fc chimera as investigated by flow cytometry (data not shown). To determine the contribution of P-selectin expressed at the cellular level to MV3 cell binding, experiments on HUVECs were carried out using a function-blocking P-selectin mAb. A slight, statistically not significant decrease in cell adhesion could be observed upon P-selectin blockade, which indicates that P-selectin is of minor relevance regarding the MV3/HUVEC interaction. This fact is of special importance for our inhibition studies on heparins, since endothelial P-selectin is another target of heparin action (3).

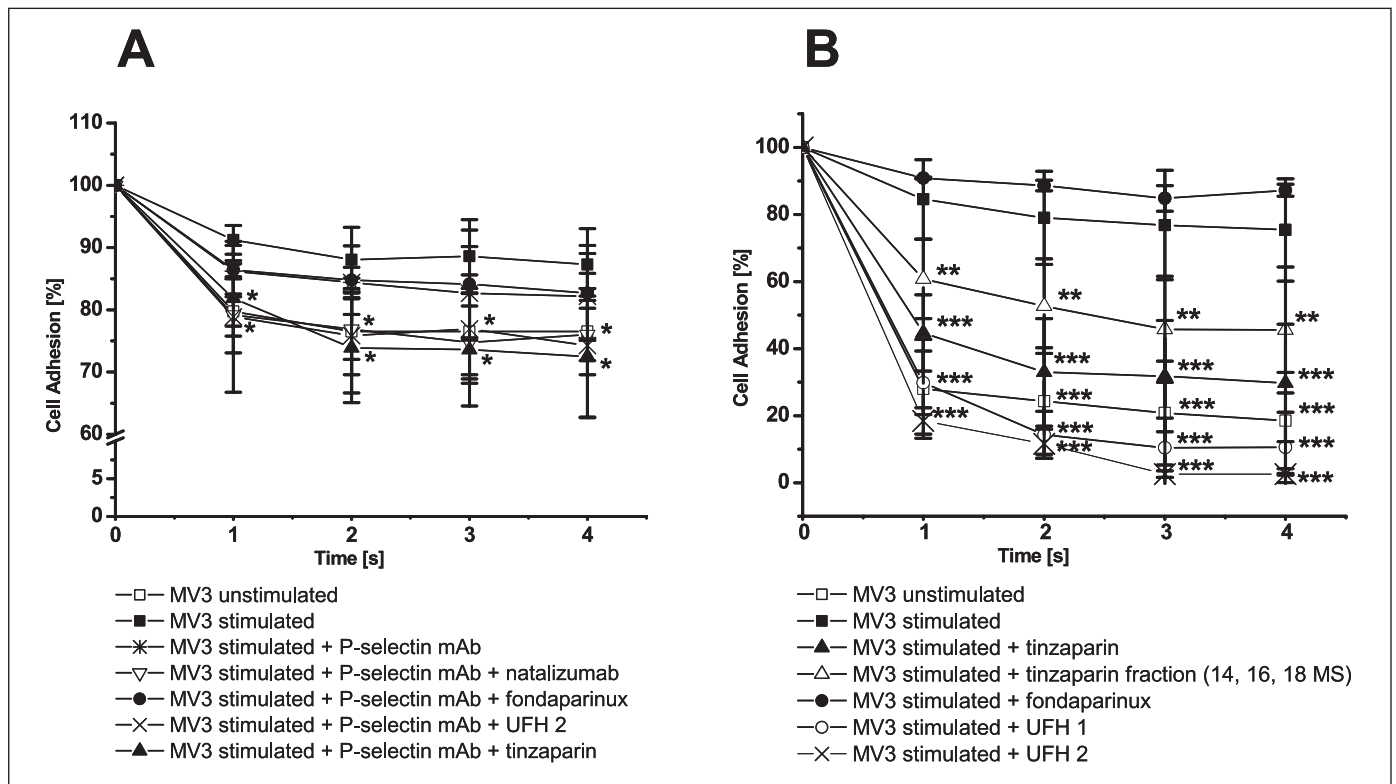


**Figure 1: Inhibition of VLA-4-mediated MV3 cell binding by heparin.** A) Adhesion of  $1 \times 10^6$   $Mn^{2+}$ -stimulated MV3 cells to confluent HUVECs under flow conditions was determined after preincubation of the cells with 500  $\mu$ g of the indicated heparins and 5  $\mu$ g natalizumab, resp., for 5 min. In some cases, the influence of a function-blocking P-selectin mAb was investigated by adding 10  $\mu$ g of the mAb to  $1 \times 10^6/100$   $\mu$ L MV3 cell suspension prior to injection into the flow system. After 5

min of sedimentation, the flow was started and the adhesion behavior was monitored over the indicated time range. B) Influence of different heparins and heparin fractions on MV3 cell adhesion to immobilised VCAM-1 under flow conditions was determined as described above. Data are presented as mean values  $\pm$  SD ( $n^3$ ; \* $p < 0.05$ , \*\* $p < 0.01$ , \*\*\* $p < 0.001$  with respect to stimulated MV3 cells). MS, monosaccharide; UFH, unfractionated heparin.

However, to rule out any P-selectin-mediated cell adhesion, inhibition studies on HUVECs were performed at concomitant application of the P-selectin mAb. The effects of different heparin preparations were analysed after a preincubation period of 5 min with stimulated cells according to our previous investigations (6). Figure 1A illustrates that both UFH 2 and tinzaparin were able to reduce cell adhesion ( $74.3\% \pm 11.6\%$  and  $72.5\% \pm 9.7\%$ , resp.) to the same extent as natalizumab in the presence of the P-selectin mAb. In contrast, fondaparinux failed to further decrease cell adhesion. These results reveal that heparin blocks VLA-4-mediated MV3 cell binding under physiological conditions using an endothelial cell layer. However, the observed inhibitory effects are relatively weak and probably hindered by unspecific binding events, which impede the determination of clear structure-activity relationships.

Thus, further inhibition studies were performed on immobilised VCAM-1 Fc chimera allowing to focus more closely on the involvement of VLA-4 (Fig. 1B). As observed for the adhesion experiments on HUVECs,  $Mn^{2+}$ -treatment led to an increase of percentaged cell adhesion, which is much more pronounced on the isolated ligand. We initially used tinzaparin, which also displayed a high inhibition capacity regarding P- and L-selectin (30). Tinzaparin reduced the MV3 cell adhesion to isolated

VCAM-1 in a statistically significant manner. It is known that tinzaparin contains more high molecular weight heparin fragments than other LMWHs. In order to investigate whether molecular weight of heparin has an impact on the blocking capacity of VLA-4/VCAM-1 interaction, two UFHs and the pentasaccharide fondaparinux have been applied. Preincubation of cells with each of the UFHs decreased cell adhesion stronger than tinzaparin, while fondaparinux revealed no inhibitory effect. Although it is not clear, which saccharide component is responsible for VLA-4 inhibition, a correlation between molecular size and inhibitory efficiency might be assumed. Moreover, exceeding a critical size appears as essential for inhibition. Since a smaller tinzaparin fraction (MW 5,600 Da compared to 6,500 Da of tinzaparin) representing only fragments of 14, 16, and 18 monosaccharides displayed significant activity (slightly reduced compared to tinzaparin), the critical threshold of heparin size seems to be between five and 14 monosaccharides. In further investigations, even smaller heparin fractions should be applied to further focus on this aspect, as well as UFH derivatives differing in sulfation or *N*-acetylation to obtain more information on the heparin binding epitope to VLA-4.

Our findings on size dependency correspond to others, who were able to show that only certain heparin fractions inhibit the

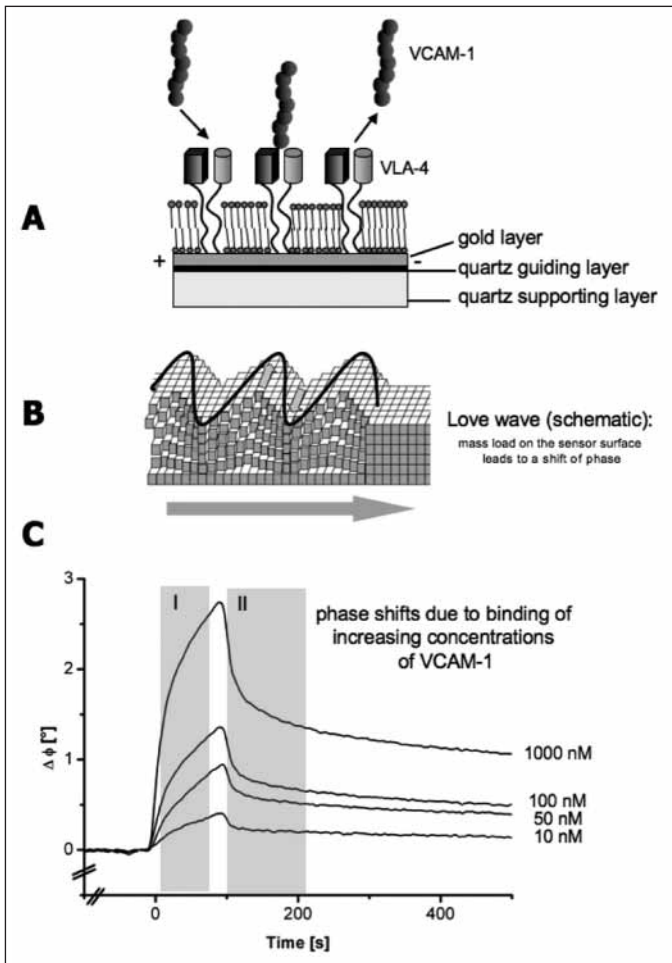


**Figure 2: Detection of kinetic binding constants using a SAW biosensor.** A) A VLA-4 containing membrane preparation was immobilised on the surface of a SAW sensor chip. VCAM-1 was injected under flow to bind to VLA-4. B) The applied voltage induces an acoustic love wave in the guiding layer of the sensor chip. The phase of this wave depends on the mass load on the sensor surface. Binding of VCAM-1 to VLA-4 led to a phase shift. Unbinding of VCAM-1 due to buffer rinsing led to returning of the initial phase. C) Phase shift versus time diagrams for increasing concentrations of injected VCAM-1 can be analysed using a non-linear curve fitting in area I for the concentration depending association rate constant ( $k_{\text{obs}}$ ) and in area II for the dissociation rate constant ( $k_{\text{off}}$ ).  $K_{\text{obs}}$  is a function of concentration and according to the equation  $k_{\text{obs}} = k_{\text{on}} c + k_{\text{off}}$ , the association rate constant ( $k_{\text{on}}$ ) can be determined via plotting  $k_{\text{obs}}$  versus  $c$  and applying a best linear fit. The underlying mathematics are explained in detail in (17). The equilibrium dissociation rate constant ( $K_{\text{D}}$ ) is determined by  $K_{\text{D}} = k_{\text{off}}/k_{\text{on}}$ . VCAM-1, vascular cell adhesion molecule-1; VLA-4, very late activation antigen-4.

binding of integrin  $\alpha\text{X}\beta 2$  to complement fragment iC3b (15). These indications on heparin blockade of MV3 melanoma cell adhesion to a VCAM-1 substratum are in line with our previous suggestion of VLA-4 being a novel heparin target (6). However, other mechanisms might contribute to the observed heparin effects, such as inhibition of heparanase that is known to have multiple cellular effects beside ECM-degradation. For instance, Sotnikov et al. were able to demonstrate that the VLA-4-mediated binding of T-cells to ECM components and to VCAM-1 is increased in the presence of enzymatically quiescent heparanase.

This appears to be due to synergistic effects with SDF-1 $\alpha$ -induced phosphorylation of kinases implicated in integrin function (31). Consequently, inhibition of this process by heparin might result in opposed effects leading to impaired VLA-4 regulation. Additionally, the functional heparin binding domain of heparanase was shown to facilitate cell adhesion and spreading by clustering of cell surface syndecan-1 and syndecan-4 on human tumor cells as a consequence of initiating different signaling pathways (32). However, the influence of these heparanase-dependent actions by heparin might be excluded for our discrete experimental conditions using the recombinant immobilised ligand. Moreover, the integrin activation performed in the present study was chemokine-independent. Thus, our data point to a direct interaction between heparin and VLA-4.

### Biosensor-based investigation of MV3 binding

To get a deeper insight into the molecular mechanisms of MV3 binding, we applied a SAW biosensor. The principle of measurement is schematically illustrated in Figure 2. VCAM-1 Fc chimera were immobilised on the sensor surface to investigate the binding of MV3 cells. Binding of  $1 \times 10^6$  stimulated MV3 cells was measured versus binding of  $1 \times 10^6$  MV3 cells under preincubation with 500  $\mu\text{g}$  tinzaparin. Figure 3A shows that tinzaparin effectively suppressed MV3 binding to VCAM-1 in agreement with the microscopic assay.

Next, we immobilised the VLA-4 antibody natalizumab to the SAW sensor surface and detected the binding of  $1 \times 10^6$  stimulated MV3 cells as well as inhibition by tinzaparin (Fig. 3B). Assuming that an interaction between cellular VLA-4 and natalizumab is based on binding of the  $\alpha$ -subunit of VLA-4, further insight into heparin binding activity can be obtained. Thus, tinzaparin may bind directly to the  $\alpha$ -subunit of VLA-4 and cause a steric hindrance for natalizumab binding. Another possibility is the conformational change of VLA-4 after tinzaparin binding leading to a prevented binding to the  $\alpha$ -subunit allosterically. However, the data strengthen our hypothesis of direct heparin/VLA-4 interaction, since we could also exclude (i) binding of natalizumab and of tinzaparin to immobilised VCAM and (ii) binding of VCAM-1 and of tinzaparin to immobilised natalizumab. For concentrations between  $1 \times 10^{-9}$  M and  $1 \times 10^{-4}$  M neither interaction nor even unspecific binding could be detected (data not shown).

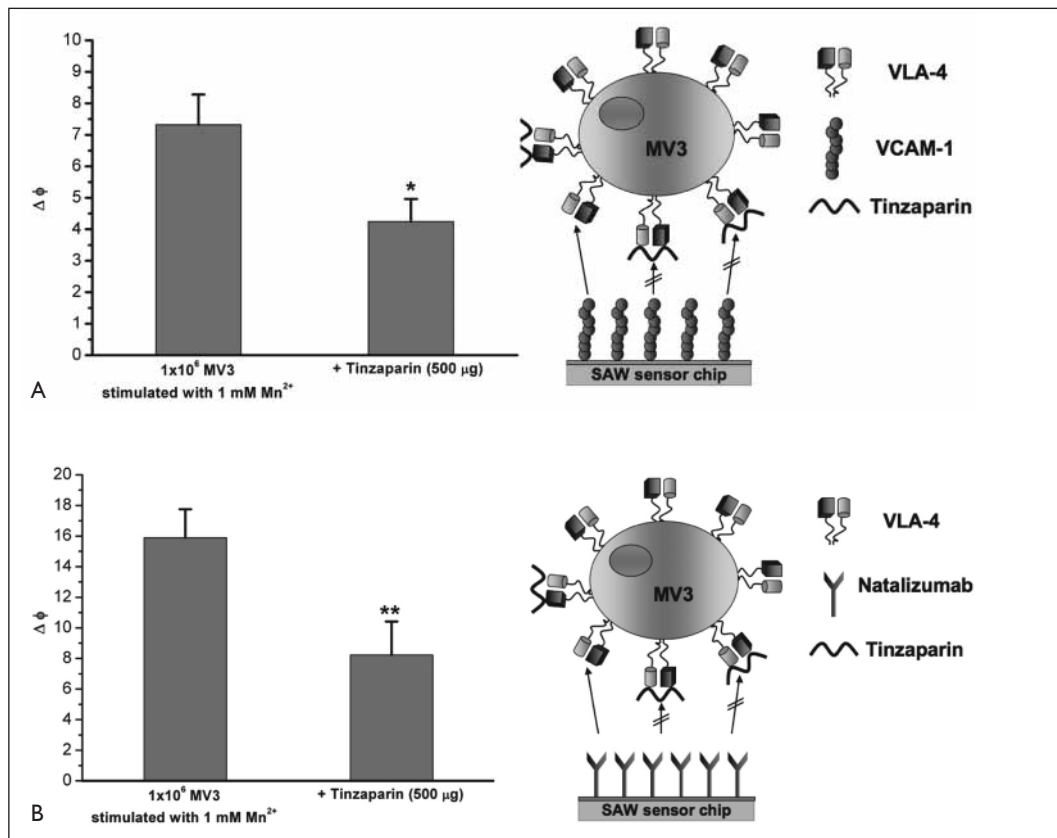
### Detection of kinetic binding constants of tinzaparin and VCAM-1 using a VLA-4 membrane preparation

In order to investigate the heparin/VLA-4 binding on a molecular level, a membrane preparation of MV3 cells was performed to obtain VLA-4-containing membrane fractions. The presence of VLA-4 in the membrane vesicles was confirmed by SDS-PAGE and Western Blot leading to bands at 280 kDa for the VLA-4 heterodimer, at 150 kDa for the  $\alpha$ -subunit and at 80 kDa, which could represent a N-terminal fragment of the  $\alpha$ -subunit (33) (data not shown). Membrane vesicles were immobilised *in situ* on a SAW sensor chip that had been prepared with a layer of 1- $\beta$ -thioglucose. Injections of increasing concentrations of VCAM-1 and tinzaparin, respectively, led to binding events that were analysed by non-linear curve fitting based on a monomolecular growth model. An exponential decay model for the deter-

### Figure 3: Inhibition of MV3 cell binding by tinzaparin in a SAW biosensor assay.

A) VCAM-1 was immobilised to gold-coated SAW sensors by EDC/NHS chemistry.  $1 \times 10^6$  MV3 cells bound to VCAM-1 after stimulation by 1 mM  $Mn^{2+}$  indicated by the phase shift due to a mass load at the sensor surface. Addition of 500  $\mu$ g tinzaparin inhibited binding of MV3 cells inducing a significant lower phase shift.

B) In an identical experimental setting, natalizumab instead of VCAM-1 was immobilised. Natalizumab binds highly specific to the  $\alpha$ -subunit of VLA-4. Tinzaparin induced a significant inhibition of MV3 cell binding to natalizumab, which might indicate a specific interaction of tinzaparin with the  $\alpha$ -subunit of VLA-4. Data are presented as means  $\pm$  SD ( $n > 3$ ; \* $p < 0.05$ , \*\* $p < 0.01$ ). SAW, surface acoustic wave; VCAM-1, vascular cell adhesion molecule-1; VLA-4, very late activation antigen-4.



mination of the corresponding binding kinetics was assumed (Table 1).

We were able to detect kinetic constants of VCAM-1 binding to VLA-4 in a biosensor assay for the first time. The binding affinity in the mean nanomolar range is obvious for a cell adhesion receptor. The rapid association rate constant confirms the potency of this interaction as a mediator of leukocyte rolling in the process of cellular immune response. The dissociation rate constant is slower than the  $k_{off}$  of the selectins (e.g.  $k_{off} = 1.4 \text{ s}^{-1}$  for P-selectin/PSGL-1 interaction (34)) and refers to the role of VLA-4 to slow down the rolling and to initialise firm adhesion. The only data available for VLA-4/VCAM-1 interaction are published by Chigaev et al. (35). They determined  $K_D$  values between  $3.31 \times 10^{-8} \text{ M}$  and  $48.9 \times 10^{-8} \text{ M}$  depending on activation with  $Mn^{2+}$  and  $Ca^{2+}$  using VLA-4-positive U937 cells and fluorescently-labelled VCAM-1 in flow cytometry experiments. They postulated that affinity changes drive change of VLA-4 avidity most importantly and could also show that intracellular activation as well as shear forces mainly affected the dissociation rate leading to different affinities. Although our approach is neither cell-based nor can it be influenced by  $Mn^{2+}$ ,  $Ca^{2+}$  or shear forces due to lacking signaling pathways, the obtained data are in good accordance with these findings. Thus, the kinetic data of VLA-4/VCAM-1 interaction have to be regarded as affinity data for one single activation state of VLA-4 and have to be compared to the data of tinzaparin.

Tinzaparin binds to VLA-4 with an affinity in the low micromolar range, which clearly indicates a specific molecular recognition. The data underscore the potency of tinzaparin as an in-

hibitor of VLA-4-mediated interactions. Although tinzaparin binds VLA-4 with a hundredfold slower association rate constant than VCAM-1, it displays a nearly identical dissociation rate constant. This appears as an important aspect with respect to inhibitory capacity, since the dissociation rate constant was shown to correlate with inhibition in case of the selectins (36). Since the pentasaccharide fondaparinux could neither show an effect in the

**Table 1: Kinetic binding constants of VCAM-1 and tinzaparin binding to VLA-4 in an immobilised membrane preparation.**

Data were extracted from sensor signals of injections of increasing concentrations of VCAM-1 and Tinzaparin using the monomolecular growth model. Binding kinetics were determined assuming an exponential decay model via non-linear curve fitting using Origin7.5TM (Additive, Friedrichsdorf, Germany).  $K_{obs}$  values extracted from the ascending part of the sensor signals for every concentration and were plotted versus concentrations of VCAM-1 and tinzaparin, resp. A linear best fit was applied to the data using the equation  $k_{obs} = k_{on} \cdot c + k_{off}$  with  $k_{on}$  = association rate constant (on-rate) and  $k_{off}$  = dissociation rate constant (off-rate),  $c$  = concentration of the injected analyte. Data are presented as means  $\pm$  SD ( $n > 3$ ).

	$K_D$ [M]	$k_{on}$ [ $M^{-1}s^{-1}$ ]	$k_{off}$ [ $s^{-1}$ ]
<b>VCAM-1</b>	$1.01 \times 10^{-8}$ $\pm 0.90 \times 10^{-8}$	$3.53 \times 10^5$ $\pm 0.57 \times 10^5$	$3.44 \times 10^{-3}$ $\pm 2.95 \times 10^{-3}$
<b>Tinzaparin</b>	$4.61 \times 10^{-6}$ $\pm 2.68 \times 10^{-6}$	$1.27 \times 10^3$ $\pm 0.58 \times 10^3$	$5.13 \times 10^{-3}$ $\pm 1.56 \times 10^{-3}$
<b>Fondaparinux</b>	n.d.	n.d.	n.d.

Key: n.d., not detectable.

cell rolling assay nor binding could be detected in the SAW assay, the specific recognition of tinzaparin by VLA-4 is confirmed.

In summary, following a recent hypothesis of inhibiting VLA-4-mediated cell binding by heparin, this study provides the first clear indication that a LMWH binds directly to VLA-4 with an affinity in a low micromolar range. Although a clear size-dependency could be obtained, further experiments using modified heparins are necessary to evaluate structural requirements of this recognition process. These results focus the interest on VLA-4 as a novel target for heparin in antimetastatic approaches and should be considered as worthwhile to continue research in this field.

## Acknowledgements

UFH 1 and the isolated tinzaparin fraction were kindly provided by Prof Dr Benito Casu and Dr Annamaria Naggi. We thank Dr Thomas Gronewold for helpful discussions regarding the biosensor application.

## References

- Schmidmaier R, Baumann P. ANTI-ADHESION evolves to a promising therapeutic concept in oncology. *Curr Med Chem* 2008; 15: 978–990.
- Borsig L, Wong R, Hynes RO, et al. Synergistic effects of L- and P-selectin in facilitating tumor metastasis can involve non-mucin ligands and implicate leukocytes as enhancers of metastasis. *Proc Natl Acad Sci U S A* 2002; 99: 2193–2198.
- Ludwig RJ, Boehme B, Podda M, et al. Endothelial P-selectin as a target of heparin action in experimental melanoma lung metastasis. *Cancer Res* 2004; 64: 2743–2750.
- Okahara H, Yagita H, Miyake K, et al. Involvement of very late activation antigen 4 (VLA-4) and vascular cell adhesion molecule 1 (VCAM-1) in tumor necrosis factor alpha enhancement of experimental metastasis. *Cancer Res* 1994; 54: 3233–3236.
- Schadendorf D, Heidel J, Gawlik C, et al. Association With Clinical Outcome of Expression of VLA-4 in Primary Cutaneous Malignant Melanoma as Well as P-selectin and E-selectin on Intratumoral Vessels. *J Natl Cancer Inst* 1995; 87: 366–371.
- Fritzsche J, Simonis D, Bendas G. Melanoma cell adhesion can be blocked by heparin in vitro: Suggestion of VLA-4 as a novel target for antimetastatic approaches. *Thromb Haemost* 2008; 100: 1166–1175.
- Liang S, Dong C. Integrin VLA-4 enhances sialyl-Lewisx/a-negative melanoma adhesion to and extravasation through the endothelium under low flow conditions. *Am J Physiol Cell Physiol* 2008; 295: C701–707.
- Akl EA, van Doormaal FF, Barba M, et al. Parenteral anticoagulation may prolong the survival of patients with limited small cell lung cancer: a Cochrane systematic review. *J Exp Clin Cancer Res* 2008; 27: 4.
- Borsig L. Selectins facilitate carcinoma metastasis and heparin can prevent them. *News Physiol Sci* 2004; 19: 16–21.
- Mousa SA, Mohamed S. Inhibition of endothelial cell tube formation by the low molecular weight heparin, tinzaparin, is mediated by tissue factor pathway inhibitor. *Thromb Haemost* 2004; 92: 627–633.
- Jayson GC, Gallagher JT. Heparin oligosaccharides: inhibition of the biological activity of bFGF on Caco-2 cells. *Br J Cancer* 1997; 75: 9–16.
- Vlodavsky I, Abboud-Jarrous G, Elkin M, et al. The impact of heparanase and heparin on cancer metastasis and angiogenesis. *Pathophysiol Haemost Thromb* 2006; 35: 116–127.
- Sobel M, Fish WR, Toma N, et al. Heparin modulates integrin function in human platelets. *J Vasc Surg* 2001; 33: 587–594.
- Diamond MS, Alon R, Parkos CA, et al. Heparin is an adhesive ligand for the leukocyte integrin Mac-1 (CD11b/CD18). *J Cell Biol* 1995; 130: 1473–1482.
- Vorup-Jensen T, Chi L, Gjelstrup LC, et al. Binding between the integrin  $\alpha X\beta 2$  (CD11c/CD18) and Heparin. *J Biol Chem* 2007; 282: 30869–30877.
- Da Silva MS, Horton JA, Wijelath JM, et al. Heparin modulates integrin-mediated cellular adhesion: specificity of interactions with alpha and beta integrin subunits. *Cell Commun Adhes* 2003; 10: 59–67.
- Perpeet M, Glass S, Gronewold TM, et al. SAW Sensor System for Marker-Free Molecular Interaction Analysis. *Anal Lett* 2006; 39: 1747–1757.
- Gronewold TM, Baumgartner A, Quandt E, et al. Discrimination of single mutations in cancer-related gene fragments with a surface acoustic wave sensor. *Anal Chem* 2006; 78: 4865–4871.
- Gronewold TM, Glass S, Quandt E, et al. Monitoring complex formation in the blood-coagulation cascade using aptamer-coated SAW sensors. *Biosens Bioelectron* 2005; 20: 2044–2052.
- Andra J, Bohling A, Gronewold TM, et al. Surface acoustic wave biosensor as a tool to study the interaction of antimicrobial peptides with phospholipid and lipopolysaccharide model membranes. *Langmuir* 2008; 24: 9148–9153.
- Deisingh AK, Thompson M. Biosensors for the detection of bacteria. *Can J Microbiol* 2004; 50: 69–77.
- Casalinuovo IA, Pierro D, Bruno E, et al. Experimental use of a new surface acoustic wave sensor for the rapid identification of bacteria and yeasts. *Lett Appl Microbiol* 2006; 42: 24–29.
- Tamarin O, Comeau S, Dejous C, et al. Real time device for biosensing: design of a bacteriophage model using love acoustic waves. *Biosens Bioelectron* 2003; 18: 755–763.
- Cavic BA, Hayward GL, Thompson M. Acoustic waves and the study of biochemical macromolecules and cells at the sensor-liquid interface. *Analyst* 1999; 124: 1405–1420.
- Hong S, Ergezen E, Barbee K, et al. BAEC adhesion analysis using Thickness Shear Mode sensor. *Conf Proc IEEE Eng Med Biol Soc* 2005; 1: 1047–1050.
- Fritzsche J, Alban S, Ludwig RJ, et al. The influence of various structural parameters of semisynthetic sulfated polysaccharides on the P-selectin inhibitory capacity. *Biochem Pharmacol* 2006; 72: 474–485.
- Lever JE. Active amino acid transport in plasma membrane vesicles from Simian virus 40-transformed mouse fibroblasts. Characteristics of electrochemical  $\text{Na}^+$  gradient-stimulated uptake. *J Biol Chem* 1977; 252: 1990–1997.
- Kaplan RS, Pedersen PL. Determination of microgram quantities of protein in the presence of milligram levels of lipid with amido black 10B. *Anal Biochem* 1985; 150: 97–104.
- Swerlick RA, Lee KH, Li LJ, et al. Regulation of vascular cell adhesion molecule 1 on human dermal microvascular endothelial cells. *J Immunol* 1992; 149: 698–705.
- Stevenson JL, Choi SH, Varki A. Differential metastasis inhibition by clinically relevant levels of heparins—correlation with selectin inhibition, not antithrombotic activity. *Clin Cancer Res* 2005; 11: 7003–7011.
- Sotnikov I, Hershkovitz R, Grabovsky V, et al. Enzymatically quiescent heparanase augments T cell interactions with VCAM-1 and extracellular matrix components under versatile dynamic contexts. *J Immunol* 2004; 172: 5185–5193.
- Levy-Adam F, Feld S, Suss-Toby E, et al. Heparanase facilitates cell adhesion and spreading by clustering of cell surface heparan sulfate proteoglycans. *PLoS ONE* 2008; 3: e2319.
- Clark K, Newham P, Burrows L, et al. Production of recombinant soluble human integrin  $\alpha 4\beta 1$ . *FEBS Lett* 2000; 471: 182–186.
- McEver RP. Selectin-carbohydrate interactions during inflammation and metastasis. *Glycoconj J* 1997; 14: 585–591.
- Chigaev A, Zwart G, Graves SW, et al.  $\alpha 4\beta 1$  integrin affinity changes govern cell adhesion. *J Biol Chem* 2003; 278: 38174–38182.
- Simonis D, Fritzsche J, Alban S, et al. Kinetic analysis of heparin and glucan sulfates binding to P-selectin and its impact on the general understanding of selectin inhibition. *Biochemistry* 2007; 46: 6156–6164.

## Abbreviations

ECM, extracellular matrix; EDC, N-ethyl-N-(dimethylaminopropyl)-carbodiimide; FCS, fetal calf serum; HUVECs, human umbilical vein endothelial cells;  $K_D$ , equilibrium dissociation constant;  $k_{off}$ , dissociation rate constant (off-rate);  $k_{on}$ , association rate constant (on-rate); LMWH, low molecular weight heparin; MS, monosaccharide; MW, molecular weight; NHS, N-hydroxysuccinimide; PBS, phosphate-buffered saline; PMNs, polymorphonuclear neutrophils; QCM, quartz crystal microbalance; SAW, surface acoustic wave; SDF-1 $\alpha$ , stromal-cell derived factor-1 $\alpha$ ; SDS, sodium-dodecylsulfate; TBS, tris-buffered saline; TFPI, tissue factor pathway inhibitor; UFH, unfractionated heparin; VCAM-1, vascular cell adhesion molecule-1; VLA-4, very late activation antigen-4.